

Near-field optical microscopy and scanning Kelvin microscopy studies of V-defects on AlGaN GaN films

C. S. Ku, J. M. Peng, W. C. Ke, H. Y. Huang, N. E. Tang, W. K. Chen, W. H. Chen, and M. C. Lee

Citation: [Applied Physics Letters](#) **85**, 2818 (2004); doi: 10.1063/1.1799248

View online: <http://dx.doi.org/10.1063/1.1799248>

View Table of Contents: <http://scitation.aip.org/content/aip/journal/apl/85/14?ver=pdfcov>

Published by the [AIP Publishing](#)

Articles you may be interested in

[Surface potential of n - and p -type GaN measured by Kelvin force microscopy](#)

Appl. Phys. Lett. **93**, 212107 (2008); 10.1063/1.3028639

[Surface band bending of a -plane GaN studied by scanning Kelvin probe microscopy](#)

Appl. Phys. Lett. **88**, 122104 (2006); 10.1063/1.2188589

[Observation of subsurface monolayer thickness fluctuations in InGaN GaN quantum wells by scanning capacitance microscopy and spectroscopy](#)

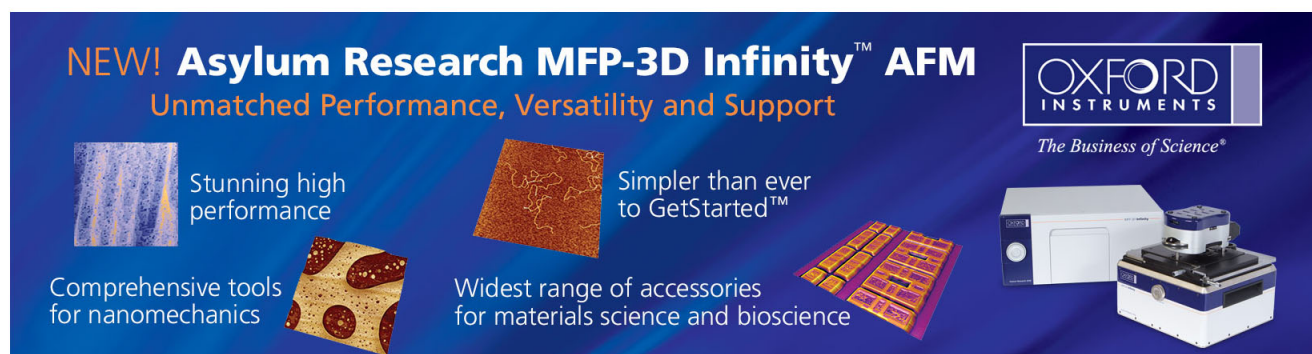
Appl. Phys. Lett. **85**, 407 (2004); 10.1063/1.1773358

[Surface and interface barriers of In x Ga 1x As binary and ternary alloys](#)

J. Vac. Sci. Technol. B **21**, 1915 (2003); 10.1116/1.1588646

[Effects of material growth technique and Mg doping on Er 3+ photoluminescence in Er-implanted GaN](#)

J. Appl. Phys. **90**, 252 (2001); 10.1063/1.1378058

The advertisement features a dark blue background with white and orange text. At the top left, it reads 'NEW! Asylum Research MFP-3D Infinity™ AFM' in large white letters, followed by 'Unmatched Performance, Versatility and Support' in orange. To the right is the Oxford Instruments logo, which includes the text 'OXFORD INSTRUMENTS' and the tagline 'The Business of Science®'. Below the main text are four images: a blue textured surface, a brown textured surface, a grid of colorful squares, and a photograph of the MFP-3D Infinity AFM instrument. Each image is accompanied by a short text description: 'Stunning high performance', 'Simpler than ever to GetStarted™', 'Comprehensive tools for nanomechanics', and 'Widest range of accessories for materials science and bioscience'.

Near-field optical microscopy and scanning Kelvin microscopy studies of V-defects on AlGa_xN/GaN films

C. S. Ku,^{a)} J. M. Peng, W. C. Ke, H. Y. Huang, N. E. Tang, W. K. Chen, W. H. Chen, and M. C. Lee

Department of Electrophysics, National Chiao Tung University, Hsinchu, 300, Taiwan, Republic of China

(Received 21 June 2004; accepted 29 July 2004)

Al_xGa_{1-x}N thin film was grown on undoped GaN/sapphire (0001) substrate by metalorganic chemical vapor deposition. V-defects were directly observed by atomic force microscopy (AFM) with various size of 0.5–2 μm in diameter. In a previous study, the microphotoluminescence spectra showed an extra peak ($I_v=350$ nm) inside the V-defect besides the near-band-edge emission ($I_{nbe}=335$ nm). To achieve better spatial resolution, we used near-field scanning optical microscopy (NSOM) and scanning Kelvin-force microscopy (SKM) to probe the V-defect in detail. The NSOM spectra showed that the intensity of the I_v band increased gradually from V-defect edges to its center, while I_{nbe} remained unchanged. Besides, the SKM measurements revealed that the Fermi level decreased from the flat region to V-defect center by about 0.2 eV. These results suggest that the I_v band could be related to shallow acceptor levels, likely resulting from V_{Ga} defects. © 2004 American Institute of Physics. [DOI: 10.1063/1.1799248]

Nitride alloys (GaN, InGaN, and AlGa_xN) are promising wide band-gap semiconductors which have applications in both electronic devices operating at high temperature, high frequency, and high power and optical devices such as light-emitting diodes in the blue-green and ultraviolet wavelength regions.^{1,2} However, for In_xGa_{1-x}N and Al_xGa_{1-x}N layers grown on GaN, an increase in In and Al compositions may inevitably cause misfit strains in films. Beyond a critical thickness, several structural defects such as misfit dislocations, stacking faults, V-shape pits, etc., are generated by plastic relaxation.³ According to the report by Wu *et al.*, the V-shape pits caused asymmetry in photoluminescence (PL) spectra with a low-energy shoulder.⁴ Our previous micro-PL studies also showed similar results.⁵ Nevertheless, these structural defects are not necessarily detrimental to their optical and electronic properties, especially for AlGa_xN films. In this letter, we present experimental results of Al_{0.16}Ga_{0.84}N by showing near-field images, electric potentials, and PL spectra of V-pits. Near-field scanning optical microscopy photoluminescence (NSOM-PL) and scanning Kelvin-force microscopy (SKM) were used to investigate the photoexcited carrier recombination mechanisms and spatial distribution of the PL spectrum. Then an energy diagram is proposed to interpret the observed transition and distribution behavior of photoexcited carriers.

The Al_{0.16}Ga_{0.84}N film was grown on the (0001) sapphire substrate at 1120 °C by using low-pressure metalorganic vapor phase epitaxy. Prior to growth, a GaN nucleation layer of 250 Å was first deposited at 520 °C, followed by a 2-μm-thick GaN buffer layer at 1120 °C. Then, the AlGa_xN layer about 0.8 μm thick was grown on GaN buffer layer at the same temperature. The Al, Ga, and N precursors were trimethylaluminum, trimethylgallium, and ammonia with flow rates of 20, 10, 5000 sccm, respectively. The electron mobility and carrier concentration were determined by Hall measurements to be 131 cm²/V s and 1 × 10¹⁸ cm⁻³, respectively. The x-ray diffraction showed the full width at half

maximum (FWHM) about 370 arcsec that is similar to the report of Choi *et al.*⁶

For NSOM-PL measurements, an atomic force microscopy (AFM, Solver P47H)-based system combined with NSOM shear-force scanner head (Solver SNC080) was employed to obtain shear-force surface topography and near field spectra. We used illumination mode, by coupling a He–Cd laser (Omnichrome 2056) operating at 325 nm with 25 mW into the single-mode quartz fiber tip that is prepared by chemical etching with HF solution, to excite the sample. The tip output power was about 100 μW and the luminescence signals were then collected by a far field micro-UV lens and coupled into a multimode fiber and sent to the monochromator (ARC-500) and photomultiplier tube (Hamamatsu R955) for detection. The tip radius of curvature is less than 100 nm as determined by SEM. It is coated with Pt of ~50 nm thickness by an ion sputter (Hitachi E-1010) in order to confine laser illumination within a very small pinhole. The distance between the fiber tip and sample surface, which was controllable and adjustable by the shear-force feedback mechanism, was usually maintained at 10–100 nm. For surface potential measurements, the SKM mode of AFM^{7,8} was employed for which the tip has a radius of curvature ~10 nm.

The AlGa_xN films grown on GaN usually contains various defects including V-shape pits. In general, the V-pit size distribution ranges from about 0.5 to 2 μm. The shear-force image in Fig. 1(a) shows one such pit of width ~1.5 μm that is common in AlGa_xN. Along one diagonal line, we measured NSOM-PL spectra at five different spots near or inside the pit except the *O* point on flat region, as shown in Fig. 1(b). At the *O* point, only the near-band-edge transition (I_{nbe}) at 335 nm is observed. From *A* to *D* points, a broad-peak (I_v) at 350 nm appears and its intensity increases from pit edge to pit center, while I_{nbe} intensity remains essentially the same. The inset of Fig. 1(b) shows the relative intensity of I_{nbe} and I_v normalized to I_{nbe} at the *O* point (flat region). In other reports^{4,9–12} the V-pit may be interpreted as the In-rich region in InGa_xN or Al-rich region in AlGa_xN. However, Al-rich or

^{a)}Electronic mail: csku.ep88g@nctu.edu.tw

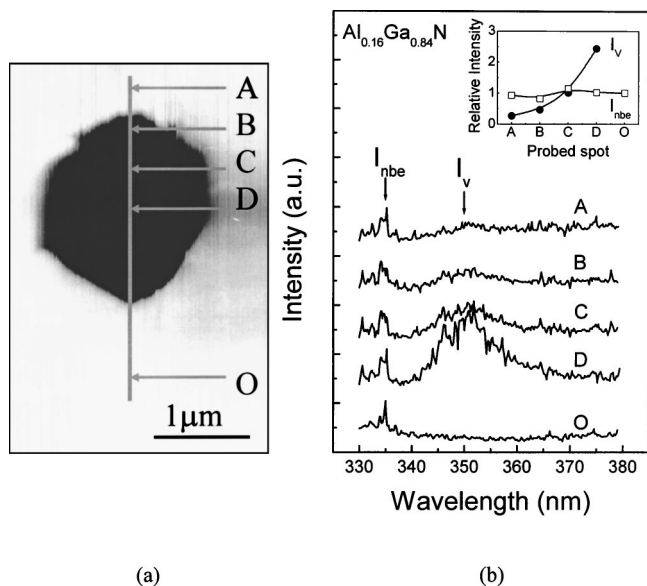


FIG. 1. (a) NSOM topography image of V-shape pit and measurement spots. (b) Near-field PL spectra taken from each spot. The inset shows that near-band-edge emission intensity changes very little but the V-pit related broad peak increased rapidly toward the pit center.

phase separation phenomena do not occur in our sample, because the I_{nbe} peak position does not change at all measured spots. Regarding the origin of the I_v peak in the V-shape pit, it may be related to the stress due to lattice mismatch between AlGa_{0.16}N and GaN films. Then, the piezoelectric field effect would cause the redshift of I_{nbe} peak position in V-shape pit of different size. However, our NSOM-PL results show insignificant shift of I_{nbe} so that it is irrelevant to the pit size. Based on our results, it is proposed that the I_v may be attributed to defect level transition.

In order to investigate the electrical potential distribution across the V-shape pit, the SKM was carried out on the same pit as that measured by NSOM. The tip-sample separation was kept at 50 nm in all measurements. As shown in Fig. 2, the AFM cross-section profile shows such a pit with $\sim 1.5 \mu\text{m}$ width and $1 \mu\text{m}$ depth. From the operational principle of SKM, an oscillating voltage $V_{\text{applied}} = V_1 \sin(\omega t)$ is applied directly to the AFM tip and combines with a dc bias voltage V_0 to detect the local surface potential. Then, the tip will feel a force of

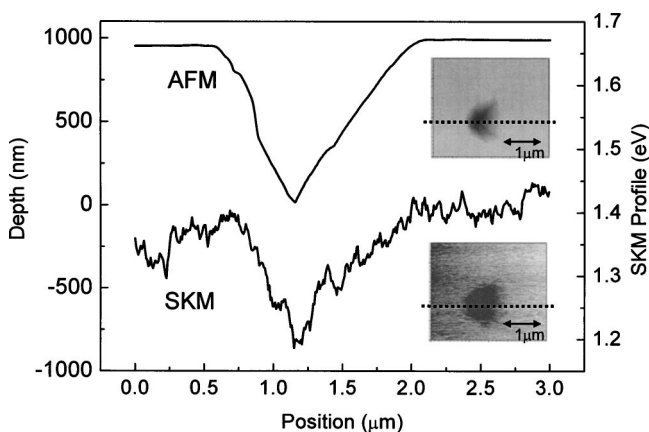


FIG. 2. The upper line show the AFM profile of V pit about $1.5 \mu\text{m}$ width and $1 \mu\text{m}$ depth. The lower line shows surface potential distribution.

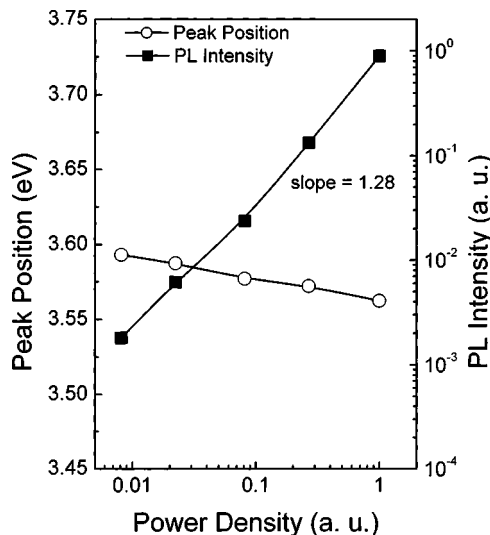


FIG. 3. Power dependence micro-PL results of peak position and intensity at 350 nm.

$$F_z(\omega) = -[(V_0 - \varphi_{x,y})V_1 \sin(\omega t)](\partial C / \partial z),$$

where $\varphi_{x,y}$ is the surface potential of sample at position (x, y) and $(\partial C / \partial z)$ is the vertical derivative of the tip-sample capacitance. The dc bias voltage is adjusted to cancel out the sample potential, i.e. $(V_0 - \varphi_{x,y}) = 0$, so that the tip feels no force. Then, $\varphi_{x,y}$ corresponds to the work function difference between the tip metal and sample, i.e., $\varphi_{x,y} = \varphi_{\text{tip}} - \varphi_{\text{AlGa}_N}$, where φ_{tip} is the work function of tip, and $\varphi_{\text{AlGa}_N} = \chi_{\text{AlGa}_N} + \xi$ is the difference between the Fermi-level and vacuum level which depends on the thickness of AlGa_{0.16}N layer.¹³ The χ_{AlGa_N} is the electron affinity and ξ is the energy difference between the Fermi level and conduction band. Thus, one can obtain the Fermi level at any position from $\varphi_{x,y}$. As shown in Fig. 2, the surface potential profile decreases from the flat region to V-pit center, and the largest potential difference is about $0.2 \pm 0.025 \text{ V}$. These results indicated that the Fermi level inside the pit is shifted toward the valence band, reflecting characteristics of acceptor type defects. Under thermal equilibrium condition, the Fermi level is assumed to be pinned at the same position, so that the band will bend upwardly inside the V-pit. Because negative charges trapped in acceptor levels and positive charges will made band bending to maintain charge neutrality. According to Jenkins *et al.* and Tansley *et al.*,^{14,15} two acceptor type levels existed below the intrinsic Fermi level in GaN, one was the antisite (Ga_N) and another was Ga vacancy (namely V_{Ga}) at 0.7–1.1 eV and 136 meV above the valence band, respectively. We tentatively attribute the I_v broad peak to the V_{Ga} -related transition, because the deep level of Ga_N cannot account for this photon energy. Jeong *et al.*,^{10,16–18} also used a similar reason to interpret the raised lower-energy shoulder in InGa_{0.16}N/GaN samples. Furthermore, we observed that the I_v peak intensity increases the excitation power with a slope of ~ 1.28 and its peak shows a small redshift of $\sim 30 \text{ meV}$ in Fig. 3. This suggests that the I_v transition should be a free-to-bound transition.

Besides, both NSOM-PL spectra and SKM surface potential profile clearly show the V_{Ga} -related defect distribution decreasing from the pit center to outer region. The dense population of V_{Ga} not only causes the Fermi level to be lower than the surrounding region, but also provides more

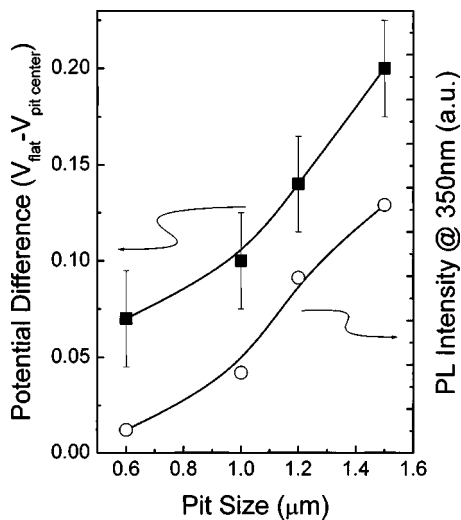


FIG. 4. Closed-square line shows the difference of the surface potential between the flat region and center of pit, indicating that the Fermi level is lower in the larger pit case. Simultaneously, the open-circle line also increased with identical trend.

recombination centers by allowing electron relaxation from shallow donor. To establish the relationship between the I_v peak intensity and pit size, we show in Fig. 4 the SKM potential difference between the pit center and the flat region and the PL intensity for different pit size. The I_v emission intensity is directly proportional to V-shape pit size in which V_{Ga} density is obviously larger. This also supports our arguments from NSOM results.

Based on the available data, we attempt to propose a schematic energy diagram. The familiar shallow donor level is responsible for the near-band-edge transition. Inside the V-shape pit, another level located at ~ 136 eV above the valence band contributes to the I_v peak. The Fermi level at the pit-center was lower than the surrounding region and carriers tend to flow to pit region for radiative recombination.

In summary, although there are only a few reports^{10,19} about spectroscopic study of V-shape pit on InGaN and GaN by using NSOM, there is no report on AlGaN yet due to poor signal collection efficiency in the UV region. We have developed an UV excitation NSOM system different from cathodoluminescence type that avoids high energy electron damage to the sample²⁰ and still provided the same spatial resolution

to investigate the V-shape pit on the $Al_{0.16}Ga_{0.84}N$ film. The results revealed the extra defect levels inside V-shape pits. In addition, the lowered Fermi level in the pit region from SKM measurements indicated new acceptor-like levels below the Fermi level. These results suggested that deep levels inside the V-pit are likely attributed to V_{Ga} -related defects. From SKM and PL studies, the V_{Ga} population is responsible for the PL intensity of different pit size and the pit formation is closely associated with V_{Ga} in AlGaN.

Grants by the National Science Council of the Republic of China under Contract Nos. NSC90-2112-M-009-040 and 89-2112-M009-056 are gratefully acknowledged.

- ¹H. Morkoc, *Nitride Semiconductors and Devices* (Springer, Heidelberg, 1999).
- ²S. Nakamura, *Science* **281**, 956 (1998).
- ³H. K. Cho, J. Y. Lee, C. S. Kim, G. M. Yang, N. Sharma, and C. J. Humphreys, *J. Cryst. Growth* **231**, 466 (2001).
- ⁴X. H. Wu, C. R. Elsass, A. Abare, M. Mack, S. Keller, P. M. Petroff, S. P. DenBaars, J. S. Speck, and S. J. Rosner, *Appl. Phys. Lett.* **72**, 692 (1998).
- ⁵H. Y. Huang, C. S. Ku, W. C. Ke, N. E. Tang, J. M. Peng, W. K. Chen, W. H. Chen, and M. C. Lee, *J. Appl. Phys.* **95**, 2172 (2004).
- ⁶S. C. Choi, J.-H. Kim, J. Y. Choi, K. J. Lee, K. Y. Lim, and G. M. Yang, *J. Appl. Phys.* **87**, 172 (2000).
- ⁷T. Mizutani, M. Arakawa, and S. Kishimoto, *IEEE Electron Device Lett.* **18**, 423 (1997).
- ⁸T. Usunami, M. Arakawa, S. Kishimoto, T. Mizutani, T. Kagawa, and H. Iwamura, *Jpn. J. Appl. Phys., Part 1* **37**, 1522 (1998).
- ⁹Y. Chen, T. Takeuchi, H. Amano, I. Akasaki, N. Yamada, and Y. Kaneko, *Appl. Phys. Lett.* **72**, 710 (1998).
- ¹⁰M. S. Jeong, Y.-W. Kim, J. O. White, E.-K. Suh, M. G. Cheong, C. S. Kim, C.-H. Hong, and H. J. Lee, *Appl. Phys. Lett.* **79**, 3440 (2001).
- ¹¹G. Pozina, J. P. Bergman, B. Monemar, T. Takeuchi, H. Amano, and I. Akasaki, *J. Appl. Phys.* **88**, 2677 (2000).
- ¹²B. Pècz, Zs. Makkai, M. A. di Forte-Poisson, F. Huet, and R. E. Dunin-Borkowski, *Appl. Phys. Lett.* **78**, 1529 (2001).
- ¹³G. Koley and M. G. Spencer, *J. Appl. Phys.* **90**, 337 (2001).
- ¹⁴D. W. Jenkins and J. D. Dow, *Phys. Rev. B* **39**, 3317 (1989).
- ¹⁵T. L. Tansley and R. J. Egan, *Phys. Rev. B* **45**, 10942 (1992).
- ¹⁶J. Elsner, R. Jones, M. I. Heiggie, P. K. Sitch, M. Haugk, Th. Freunheim, S. Oberg, and P. R. Briddon, *Phys. Rev. B* **58**, 12571 (1998).
- ¹⁷X. Li, P. W. Bohn, J. Kim, J. O. White, and J. J. Coleman, *Appl. Phys. Lett.* **76**, 3031 (2000).
- ¹⁸S. H. Yang, K. S. Nahn, Y. B. Hahn, Y. S. Lee, M. S. Jeong, and E.-K. Suh, *J. Korean Phys. Soc.* **36**, 1821 (2000).
- ¹⁹P. A. Crowell, D. K. Young, S. Keller, E. L. Hu, and D. D. Awschalom, *Appl. Phys. Lett.* **72**, 927 (1998).
- ²⁰J. L. Bubendorff, D. Pastrc, and M. Troyon, *J. Microsc.* **199**, 191 (2000).